Estimation of the critical dynamics and thickness of superconducting films and interfaces

T. Schneider*

Physik-Institut der Universität Zürich, Winterthurerstrasse 190, CH-8057 Zürich, Switzerland

(Received 22 June 2009; revised manuscript received 16 November 2009; published 8 December 2009)

We demonstrate that the magnetic field dependence of the conductivity measured at the transition temperature allows the dynamical critical exponent, the thickness of thin superconducting films and interfaces, and the limiting lateral length to be determined. The resulting tool is applied to the conductivity data of an amorphous $Nb_{0.15}Si_{0.85}$ film and a $LaAlO_3/SrTiO_3$ interface.

DOI: 10.1103/PhysRevB.80.214507 PACS number(s): 74.40.+k, 74.90.+n, 74.78.Fk

In a phase transition, sufficiently close to the transition temperature T_c, critical fluctuations are expected to dominate. The closer one gets to T_c, the longer these fluctuations will last, and the larger the relevant length scale becomes. In a superconductor the relevant length scale is the correlation length ξ. Without loss of generality we can assume that the lifetime of the fluctuations, τ, varies as $\tau \propto \xi^z$ which defines z, the dynamical critical exponent.[1,2] As we approach the critical region, all the physics that really matters is associated with the diverging length and time scales.

Using experimentally accessible quantities, voltage V and current I, dynamic scaling predicts for superconducting films and interfaces the relationship[1]

$$V = I\xi^{-z} g_{\pm}\left(\frac{I\xi}{T}\right). \tag{1}$$

$g_{\pm}(x)$ is a scaling function of its argument above (+) and below (−)T_c. Above T_c, in the limit $x \to 0$, $g_+(x)$ tends to a constant and the conductivity to

$$\sigma = \frac{I}{V} \propto \xi^z. \tag{2}$$

On the other hand, at T_c in the limit $x \to \infty$, $g_{\pm}(x)$ tends to x^z so that

$$V \propto I^{a(T_c)}, \quad a(T_c) = z + 1. \tag{3}$$

In practice I-V data exhibit resistive tails revealing finite-size-induced free vortices which make it difficult to estimate the transition temperature T_c and the dynamical scaling exponent z.[3–7]

Alternatively, the application of the conductivity relation (2) requires the explicit form of the correlation length. Since superconducting thin films and interfaces are expected to undergo a Berezinskii-Kosterlitz-Thouless (BKT) transition from the superconducting to the normal state the correlation length adopts for $T \geq T_c$ the characteristic form[8,9]

$$\xi(T) = \xi_0 \exp\left(\frac{2\pi}{bt^{1/2}}\right), \quad t = \frac{T}{T_c} - 1. \tag{4}$$

ξ_0 is related to the vortex core radius and b to the energy needed to create a vortex.[10–13] Accordingly the analysis of conductivity or resistivity data in zero magnetic field provide in terms of $\sigma \propto \xi^z$ estimates for T_c, ξ_0^z, and z/b (Refs. 14–17) while the dynamical critical exponent z cannot be determined. Furthermore, the relationship $\sigma \propto \xi^z$ allows to perform a standard finite-size scaling analysis.[17,18]

In this context it is important to recognize that the existence of the BKT transition (vortex-antivortex dissociation instability) in ^{4}He films is intimately connected with the fact that the interaction energy between vortex pairs depends logarithmic on the separation between them. As shown by Pearl,[19] vortex pairs in thin superconducting films (charged superfluid) have a logarithmic interaction energy out to the characteristic length $\lambda_{2D} = \lambda^2/d$, beyond which the interaction energy falls off as $1/r$. Here λ is the magnetic penetration depth of the bulk. As λ_{2D} increases the diamagnetism of the superconductor becomes less important and the vortices in a thin superconducting film become progressively like those in ^{4}He films.[20] According to this $\lambda_{2D} \gg \min[W,L]$ is required, where W and L denote the width and the length of the perfect sample. Invoking the Nelson-Kosterlitz relation[21] $\lambda_{2D}(T_c) = \lambda^2(T_c)/d = \Phi_0^2/(32\pi^2 k_B T_c)$ it is readily seen that for sufficiently low T_c's and $\min[W,L] \ll 1$ cm this condition is well satisfied. As a result any rounding of the transition due to finite-size effects should be more important than that due to the finite magnetic "screening length" λ_{2D}.

Here we present a tool to determine the dynamical critical exponent z, the thickness d, and the limiting length $\hat{L}$, associated with the resistive tail in zero magnetic field, from conductivity measurements taken at T_c and in magnetic fields applied parallel and perpendicular to the film or interface. Traditionally the thickness of superconducting films is estimated from the angular dependence of the upper critical field H_{c2}.[22] Noting that H_{c2} is an artifact of the mean-field approximation this approach becomes questionable in two dimensions where thermal fluctuations are enhanced. The crucial component of the tool stems from the magnetic field induced finite-size effect. For $T \geq T_c$ and nonzero magnetic field the mean distance between the vortex lines $(\Phi_0/H)^{1/2}$ is another characteristic length, preventing the correlation length to diverge at T_c and $H > 0$.[23] The resulting magnetic field induced finite-size effect can be described by relating the zero-field and finite-field correlation length in terms of

$$\xi_x(T,H_z)\xi_y(T,H_z) = \xi_x(T,0)\xi_y(T,0)G(x), \tag{5}$$

where

$$x = \frac{aH_z\xi_x(T,0)\xi_y(T,0)}{\Phi_0} = \frac{\xi_x(T,0)\xi_y(T,0)}{L_{H_z}^2},$$

$$L_{H_z}^2 = \frac{\Phi_0}{aH_z}. \tag{6}$$

L_{H_z} is the limiting magnetic length and $G(x)$ denotes the finite-size scaling function with the limiting behavior,

$$G(x) = \begin{cases} 1 : x = 0 \\ 1/x : x \to \infty \end{cases}. \tag{7}$$

Indeed, in zero field the limiting magnetic length L_{H_z} is infinite and the growth of the correlation length ξ is unlimited while in finite fields the divergence of ξ at T_c is removed and its value is given by

$$\xi_x(T_c,H_z)\xi_y(T_c,H_z) = L_{H_z}^2 = \frac{\Phi_0}{aH_z}, \tag{8}$$

where a fixes the mean distance between vortices. The equivalence to the standard finite-size effect in a film of dimensions $L\times L$ is readily established by noting that in this case the correlation length scales as $\xi(T,L)=\xi(T,L=\infty)G[\xi(T,L=\infty)/L]$.[18]

More generally in magnetic fields $H_{\perp,\parallel}$, applied perpendicular ($\perp$) or parallel ($\parallel$) to the film or interface, the divergence of $\xi(T)$ at T_c is then removed because $\xi(T_c)$ cannot grow beyond

$$\tilde{L} = \begin{cases} \hat{L} \\ L_{H_\perp} = \left(\dfrac{\Phi_0}{aH_\perp}\right)^{1/2} \\ L_{H_\parallel} = L_{H_\parallel} = \dfrac{\Phi_0}{aH_\parallel d} \end{cases}. \tag{9}$$

Here we included the limiting length $\hat{L}$ arising from the ohmic tail in zero field, e.g., due to the system size or the finite lateral extent of the homogenous domains. The expressions for the magnetic field induced limiting lengths $L_{H_\perp}$ and $L_{H_\parallel}$ follow from Eq. (8) and by noting that the correlation lengths of fluctuations which are transverse to the applied magnetic field are bounded according to $\xi_x\xi_y \leq \Phi_0/(aH_x)$, $x\neq y\neq z$, where $\xi_z=d$, $H_\perp=H_z$, $H_x=H_y=H_\parallel$, and accordingly $\xi_x\xi_y=\xi_\parallel^2\leq L_{H_\perp}^2=\Phi_0/aH_\perp$ and $\xi_x\xi_z=\xi_\parallel d\leq L_{H_\parallel}d=\Phi_0/aH_\parallel$, where d denotes the film thickness.

These limiting lengths prevent the divergence of the conductivity at T_c. In zero field it adopts according to Eqs. (2) and (9) the form

$$\sigma(T_c,H_{\perp,\parallel}=0) = f\hat{L}^z. \tag{10}$$

As the magnetic field increases this behavior applies as long as $\hat{L}<L_{H_{\perp,\parallel}}$ while for $\hat{L}>L_{H_{\perp,\parallel}}$ the magnetic field sets the limiting length and the conductivity approaches according to Eqs. (2) and (9) the form

$$\sigma(T_c,H_{\perp,\parallel}) = \sigma_n + \begin{cases} f_\perp H_\perp^{-z/2}, & f_\perp = f(\Phi_0/a)^{z/2} \\ f_\parallel H_\parallel^{-z}, & f_\parallel = f(\Phi_0/ad)^z \end{cases}, \tag{11}$$

where σ_n is the normal-state conductivity, attained in the high-field limit. The thickness d of the superconducting film or interface follows then from

$$d^2 = \frac{\Phi_0}{a}\left(\frac{f_\perp}{f_\parallel}\right)^{2/z}, \tag{12}$$

whereby an estimation of d requires the value of the dynamical critical exponent z, derivable from the magnetic field dependence of the conductivity at T_c [Eq. (11)]. So far we concentrated on temperatures at and above the BKT transition. Below T_c the correlation length diverges, $\xi\to\infty$.[8,9] This implies that ξ will be cut off by a limiting length and with that are Eqs. (10) and (11) expected to apply for $0<T\leq T_c$. Since the low-temperature phase in the BKT scenario is described by a line of fixed points, each temperature $T<T_c$ may be characterized by its own $f(T)$.

An essential assumption of the outlined approach is the dominance of thermal phase fluctuations around T_c. There is considerable evidence for a critical magnetic field $H_{\perp,\parallel c}$, emerging from a nearly temperature-independent crossing point in the resistance-magnetic field plane.[24–31] It can be identified as the critical field of the quantum superconductor to insulator (QSI) transition and the resistance is predicted to scale as $R(H_{\perp,\parallel},T)=R_c f(|H_{\perp,\parallel}-H_{\perp,\parallel c}|/T^{1/\bar{z}\bar{\nu}})$,[32] where $\bar{\nu}$ is the zero-temperature correlation length exponent and $\bar{z}$ is the quantum dynamical critical exponent. However, recent experiments[30,33] that have explored the competition between thermal and quantum fluctuations at low enough temperatures revealed that a temperature-independent critical field occurs at low temperatures only, where quantum fluctuations are no longer negligible.

To illustrate this tool, allowing z, d, and $\hat{L}$ to be determined from the magnetic field dependence of the conductivity at T_c we analyze next the data of Aubin *et al.*[30] of an amorphous 125-Å-thick $Nb_{0.15}Si_{0.85}$ film. In Fig. 1(a) we depicted the temperature dependence of the sheet resistance in zero field to estimate T_c and to uncover a rounded transition attributable to a finite-size effect. Evidence for characteristic BKT behavior emerges from the inset showing $[d\ln(R)/dT]^{-2/3}$ vs T in terms of the consistency with $[d\ln(R)/dT]^{-2/3}=(2/b_R)^{2/3}(T-T_c)$ in an intermediate temperature regime above T_c. The resulting estimates for b_R and T_c are then used to obtain the BKT resistance, $R=R_0\exp[-b_R/(T-T_c)^{1/2}]$, by adjusting R_0 in this intermediate regime ($0.23\lesssim T\lesssim 0.34$ K). The comparison between the resulting solid BKT line and the data reveals a rounded transition and with that a finite-size effect generating free vortices at and below $T_c=0.224$ K. In this context we note that according to the Harris criterion weak randomness in the local T_c, pairing interaction, etc., does not change the critical BKT behavior.[34] Nevertheless, inhomogeneities due to local strain or a heat current appear to be likely in both, superconducting films and interfaces. A nonzero heat current drives the system away from equilibrium. A temperature gradient is created which implies that the temperature is space dependent.

To substantiate and complete the consistency with limited BKT behavior in zero field we perform a finite-size scaling analysis.[17,18] Supposing that there is a limiting length $\hat{L}$ preventing the correlation length to grow beyond $\hat{L}$ finite-size scaling implies that $R(T,\hat{L})$ scales as

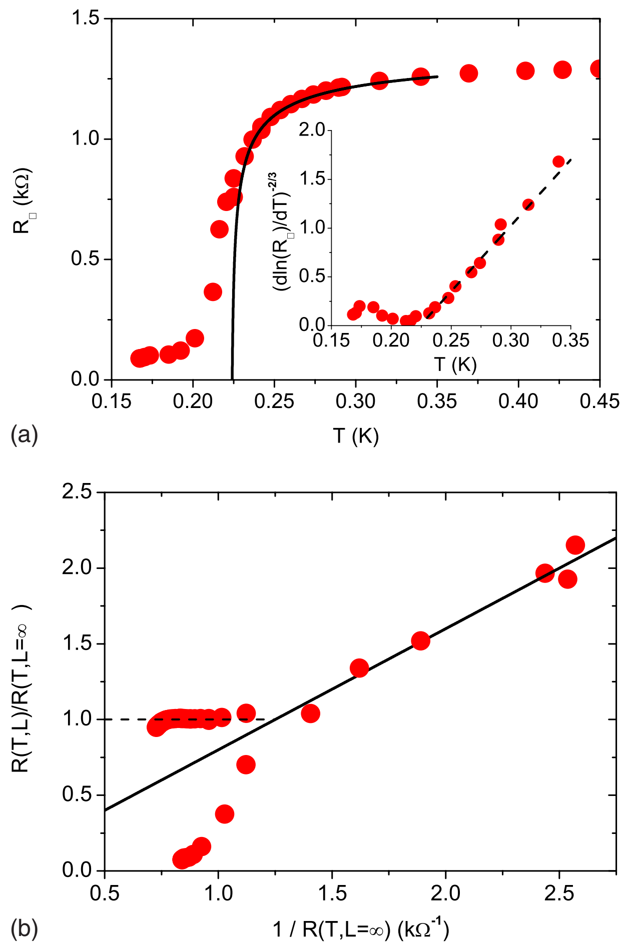

FIG. 1. (Color online) (a) $R_{\square}(T)$ of an amorphous 125-Å-thick $Nb_{0.15}Si_{0.85}$ film taken from Aubin *et al.* (Ref. 30). The solid line is $R = R_0 \exp[-b_R/(T-T_c)^{1/2}]$ with $R_0 = 1.41\ \text{k}\Omega$, $b_R = 0.0403\ \text{K}^{1/2}$, and $T_c = 0.224\ \text{K}$. The inset shows $[d\ln(R)/dT]^{-2/3}$ vs T and the dashed line is $[d\ln(R)/dT]^{-2/3} = (2/b_R)^{2/3}(T-T_c)$. (b) $R(T,\hat{L})/R(T,L=\infty)$ vs $1/R(T,\hat{L}=\infty)$, where $R(T,\hat{L}=\infty) = R_0 \exp(-b_R/|T-T_c|^{1/2})$ and $R(T,\hat{L})$ denotes the experimental data. The upper branch corresponds to $T > T_c$ and the lower one to $T < T_c$. The dashed line is $R(T,L) \simeq R(T,\infty)$ and the solid one $R(T,\hat{L}) = g(\hat{L}) = g/\hat{L}^2$ with $g(\hat{L}) \simeq 800$.

$$\frac{R(T,\hat{L})}{R(T,\hat{L}=\infty)} = \left[\frac{\xi(T,0)}{\xi(T,\hat{L}=\infty)}\right]^2 = g(x), \tag{13}$$

where

$$x = \frac{1}{R(T,\hat{L}=\infty)\hat{L}^2} \propto \left[\frac{\xi(T,\hat{L})=\infty}{\hat{L}}\right]^2. \tag{14}$$

$g(x)$ is the finite-size scaling function adopting in the present case the limiting behavior,

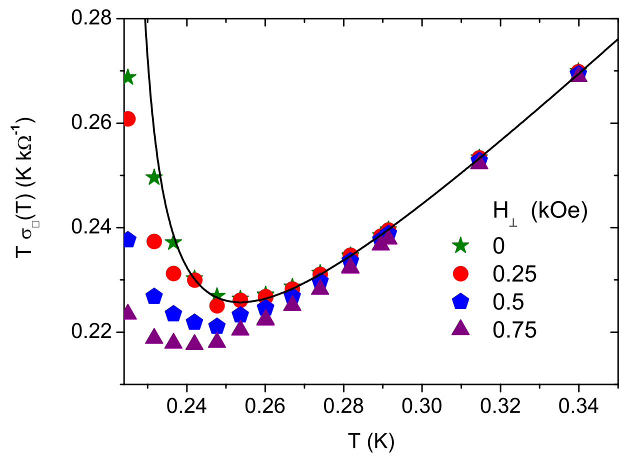

FIG. 2. (Color online) $T\sigma(T,H_{\perp})$ vs T for various $H_{\perp}$ for an amorphous 125 Å thick $Nb_{0.15}Si_{0.85}$ film derived from Aubin *et al.* (Ref. 30). The solid line is $T\sigma(T,H_{\perp}) = T/R = (1/R_0)\exp[b_R/(T-T_c)^{1/2}]$ with $R_0 = 1.41\ \text{k}\Omega$, $b_R = 0.0403\ \text{K}^{1/2}$, and $T_c = 0.224\ \text{K}$.

$$g(x) = \begin{cases} 1 : \xi(T,\infty) \ll \hat{L} \\ gx : \xi(T,\infty) \gg \hat{L} \end{cases} . \tag{15}$$

BKT behavior, $R(T,\hat{L}) = R(T,\hat{L}=\infty)$, is then observable as long as $\xi(T,\infty) < \hat{L}$ while for $\xi(T,\infty) > \hat{L}$ the scaling function approaches

$$R(T,\hat{L}) = g(\hat{L}) = g/\hat{L}^2. \tag{16}$$

A glance at Fig. 1(b) reveals that the zero-field data shown in Fig. 1(a) are fully consistent with BKT critical behavior in a finite system of lateral extent $\hat{L}$. In particular, the tail below $T_c \simeq 0.224\ \text{K}$ was traced back to a finite-size effect. Furthermore, above T_c and for asymptotically small fields the magnetic susceptibility $\chi_{\perp} = m(T,H_{\perp})/H_{\perp} = -\xi^2[k_B T/(2d\Phi_0^2)]$ (Ref. 35) and the conductivity, $\sigma(T,H_{\perp}=0) \propto \xi^z(T,H_{\perp}=0)$ [Eq. (2)] are related by

$$\chi_{\perp} \propto -\frac{k_B T}{2d\Phi_0^2}\sigma^{2/z}(T,H_{\perp}=0). \tag{17}$$

Accordingly, the occurrence of finite-size-limited BKT behavior can also be inferred from the magnetic susceptibility and the conductivity. In Fig. 2 we depicted $T\sigma(T,H_{\perp})$ vs T derived from the data of Aubin *et al.*[30] in the field and temperature range where Eq. (17) is expected to apply. The solid line is the characteristic BKT behavior in terms of $T\sigma(T,H_{\perp}=0)$ vs T resulting from the finite-size scaling analysis. As expected, pronounced deviations occur close to $T_c \simeq 0.224\ \text{K}$, where ξ is prevented to diverge due to the limiting lengths $\hat{L}$ or $L_{H_{\perp}} = [\Phi_0/(aH_{\perp})]^{1/2}$ [Eq. (9)]. Nevertheless, in the temperature regime $(0.23 \lesssim T \lesssim 0.35\ \text{K})$, where the magnetic field induced finite-size sets the limiting length $L_{H_{\perp}}$ the data flows with reduced $H_{\perp}$ to the characteristic zero-field BKT behavior because $L_{H_{\perp}}$ increases. On the contrary, at T_c and $H_{\perp}=0$, where $L_{H_{\perp}}$ is infinite the data clearly uncovers that the divergence of ξ is eliminated by the limiting length $\hat{L}$. Invoking the detailed finite-size scaling analysis of the zero-field resistance and the low-field dependence of the conductivity we identified an intermediate temperature regime uncovering consistency with the characteristic BKT behavior in the intermediate temperature regime $0.23 \lesssim T \lesssim 0.34$ K above $T_c \simeq 0.224$ K. In addition, we detected the limiting lateral length $\hat{L}$, preventing the divergence of the correlation length by approaching T_c. Nevertheless, the outlined finite-size analysis allowed to estimate T_c of the fictitious infinite and homogeneous system reliably. The verification of BKT behavior also implies that in this temperature regime the phase fluctuations of the order parameter dominate and the expectation value of the absolute value of the order-parameter squared remains finite.

In this context it is important to note that the adopted BKT scenario requires that the temperature window $T_{c0}-T_c$, where T_{c0} denotes the BCS mean-field transition temperature, is sufficiently large. T_{c0} can be estimated from the contribution of Gaussian fluctuations to the sheet conductance, $\sigma=\sigma_n+\tilde{\sigma}_0/(T/T_{c0}-1)$, where σ_n is the normal-state sheet conductivity and $\tilde{\sigma}_0=\pi e^2/8h \simeq 1.52\times 10^{-5}\ \Omega^{-1}$.[36] A fit of this equation to the resistance data between 0.28 and 3 K, partially shown in Fig. 1(a), yields $R_n \simeq 1.315$ kΩ and $T_{c0} \simeq 0.3$ K compared to $T_c \simeq 0.224$ K. Accordingly, fluctuation effects should be observable below $T_{c0} \simeq 0.3$ K, in agreement with Fig. 1. In order to attribute the shift $T_c/T_{c0} \simeq 0.75$ to BKT fluctuations it remains to be shown that the shift due to Gaussian fluctuations, $(T_{cg}-T_{c0})/T_{c0} = 2Gi\ \ln(4Gi)$,[37] is considerably smaller. T_{cg} is the transition temperature, renormalized with respect to Gaussian fluctuations and $Gi \simeq (e^2/23\hbar)R_n$ is the Ginzburg-Levanyuk parameter for a dirty film. Using $R_n \simeq 1.315$ kΩ we obtain $Gi \simeq 0.014$ and with that $T_{cg}/T_{c0} \simeq 0.92$, revealing that Gaussian fluctuations cannot account for the observed finite-size-limited critical behavior emerging from Fig. 1. As the tool relies on a reliable estimate of T_c it applies to sufficiently homogeneous films with a limiting length such that the BKT critical regime is accessible. On the other hand, an analysis based on the Gaussian approximation provides an estimate for R_n and with $Gi \propto R_n$ a measure for the strength of fluctuations.

Next we turn to a detailed analysis of the effects of an applied magnetic field, inducing additional free vortices. In Fig. 3 we show the sheet conductivity $\sigma_\square(T_c)$ vs $H_\perp$ derived from the resistivity data. Above $H_\perp^* = 1.75$ kOe we observe for

$$z \simeq 2 \tag{18}$$

consistency with $\sigma(T_c,H_\perp)=\sigma_n+f_\perp H_\perp^{-z/2}$ [Eq. (11)] and therewith evidence for diffusive dynamics.[1] In the low-field limit deviations from Eq. (11) are expected because for sufficiently low $H_\perp$ the magnetic length $L_{H_\perp}=(\Phi_0/aH_\perp)^{1/2}$ is no longer large compared to $\hat{L}$, the zero-field limiting length.

According to Fig. 4, depicting $\sigma_\square(T_c)$ vs $H_\parallel$ of the same sample, agreement with $\sigma(T_c,H_\parallel)=\sigma_n+f_\parallel H_\parallel^{-z}$ [Eq. (11)] is obtained above $H_\parallel^*=6$ kOe for $z \simeq 2$. So this value is consistent with both the perpendicular and parallel magnetic field dependence. Given then the evidence for $z=2$ and the estimates for $f_\perp$ and $f_\parallel$ we obtain with the nominal thickness of the film, $d \simeq 125$ Å (Ref. 30) and Eq. (12) for a, fixing the mean distance between vortices, the estimate

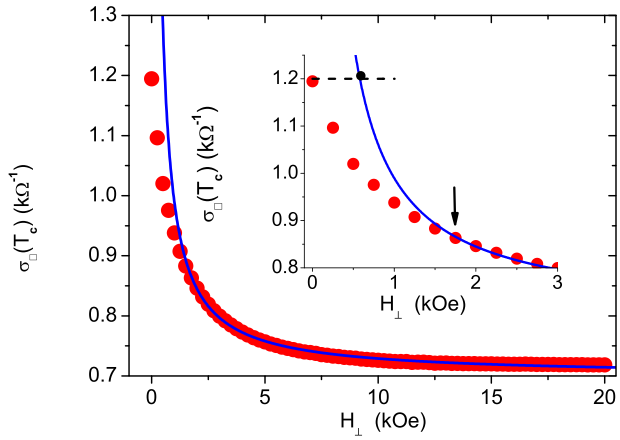

FIG. 3. (Color online) $\sigma_\square(T_c)$ vs $H_\perp$ for an amorphous 125-Å-thick $Nb_{0.15}Si_{0.85}$ film and $T \simeq 0.224$ K $\simeq T_c$ derived from Aubin *et al.* (Ref. 30). The solid line is Eq. (11) with $\sigma_n=0.70$ kΩ^{-1} and $f_\perp=0.29$ kΩ^{-1} kOe. The arrow marks $H_\perp^*=1.75$ kOe and the dot $H_\perp^\bullet=0.59$ kOe.

$$a \simeq 4.8 \tag{19}$$

compared to $a \simeq 3.12$, found in bulk cuprate superconductors.[23] Note that the film thickness was monitored *in situ* during the evaporation by a set of piezoelectric quartz. Moreover, the thicknesses and compositions were checked *ex situ* by Rutherford backscattering. The accuracy is estimated to be $\pm 5\%$.[38] In analogy to the behavior in the perpendicular field deviations from Eq. (11) occur with reduced field strength. They set in around $H_\parallel^*=6$ kOe, where $L_{H_\parallel^*}=\Phi_0/(adH_\parallel^*)$ is no longer large as compared to $\hat{L}$. To estimate $\hat{L}$ we note that Eqs. (10) and (11) imply that at $H_\parallel^\bullet$ and $H_\perp^\bullet$ (see Figs. 2 and 3) the relation

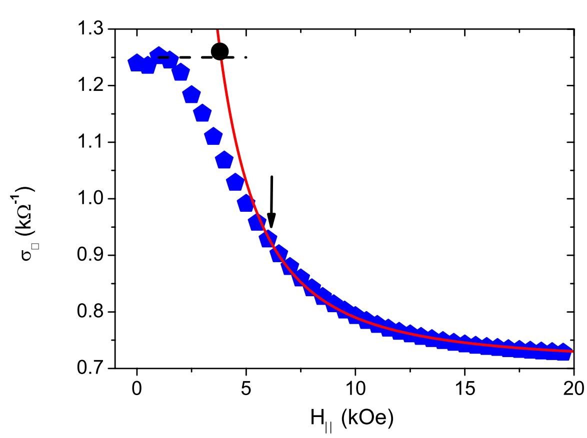

FIG. 4. (Color online) $\sigma_\square(T_c)$ vs $H_\parallel$ for an amorphous 125-Å-thick $Nb_{0.15}Si_{0.85}$ film and $T=0.224$ K $\simeq T_c$ derived from Aubin *et al.* (Ref. 30). The solid line is Eq. (11) with $\sigma_n=0.71$ kΩ^{-1} and $f_\parallel=8$ kΩ^{-1} kOe^2. The arrow marks $H_\parallel^*=6$ kOe and the dot $H_\parallel^\bullet=3.85$ kOe.

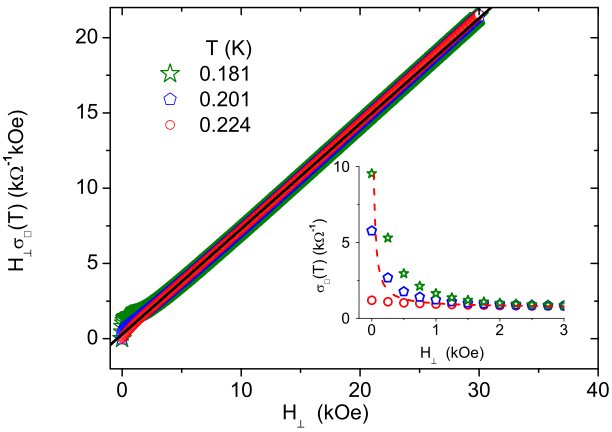

FIG. 5. (Color online) $H_\perp\sigma_\square(T)$ vs $H_\perp$ for an amorphous 125-Å-thick $Nb_{0.15}Si_{0.85}$ film at $T=0.224$ K$\simeq T_c$, $T=0.201$ K, and $T=0.181$ K derived from Aubin *et al.* (Ref. 30) The solid line is Eq. (11) in terms of $H_\perp\sigma(T_c,H_\perp)=\sigma_n H_\perp+f_\perp$ with $z=2$, $\sigma_n=0.70$ kΩ^{-1}, and $f_\perp=0.29$ kΩ^{-1} kOe. The inset shows $\sigma_\square(T)$ vs $H_\perp$. The dashed line is Eq. (11) with $\sigma_n=0.70$ kΩ^{-1} and $f_\perp=0.29$ kΩ^{-1} kOe.

$$\hat{L}=\frac{\Phi_0}{adH_\parallel^\bullet}=\left(\frac{\Phi_0}{aH_\perp^\bullet}\right)^{1/2} \tag{20}$$

holds. With $H_\perp^\bullet=0.59$ kOe and $a\simeq4.8$ we obtain $\hat{L}\simeq855$ Å while $H_\parallel^\bullet=3.85$ kOe and $d=125$ Å yields $\hat{L}\simeq896$ Å, compared to the lateral dimensions $W\times L=0.28$ cm$\times0.15$ cm of the film.[38] Invoking the Kosterlitz-Nelson relation $\lambda_{2D}(T_c)=\lambda^2(T_c)/d=\Phi_0^2/(32\pi^2k_BT_c)$ we obtain $\lambda_{2D}(T_c)\simeq4.4$ cm for $T_c=0.224$ K, whereupon $\lambda_{2D}\gg\min[W,L]$ is well satisfied for this film. Because $\lambda_{2D}(T_c)$ is also large compared to $\hat{L}$, the zero-field limiting length appears to be set by the lateral extent of the homogenous domains. In any case, the uncovered limiting length implies the presence of free vortices below T_c, precluding a true phase transition. Accordingly, the rounded BKT transition seen in Fig. 1 is traced back to a limiting length not attributable to the finite magnetic screening length λ_{2D}.

As aforementioned, below T_c the correlation length diverges.[8,9] Correspondingly, $\xi\to\infty$ will be cut off by a limiting length and Eqs. (10) and (11) are expected to apply for $T\le T_c$. Since the low-temperature phase in the BKT scenario is described by a line of fixed points, each temperature $T<T_c$ may be characterized by its own $f(T)$. To clarify this conjecture we invoke Eq. (11) in the form $H_\perp\sigma(T,H_\perp)=H_\perp\sigma_n+f_\perp(T)$ with $z=2$. The data should then fall on straight lines with slope σ_n and intercepts $f_\perp(T)$. In Fig. 5, depicting $H_\perp\sigma_\square(T)$ vs $H_\perp$ for temperatures at and below T_c, we observe that above $H_\perp^*=1.75$ kOe (see Fig. 3), where the magnetic field sets the limiting length, the data falls on a single line while below $H_\perp^*$ a crossover to the zero-field limit behavior, $\sigma(T_c,H_\perp=0)=f(T)\hat{L}^z$ [Eq. (10)] sets in. Indeed, around $H_\perp^*$ the magnetic limiting length $L_{H_\perp}$ becomes comparable to $\hat{L}$. From the inset, showing $\sigma_\square(T)$ vs $H_\perp$, it is seen that in zero field $f(T)$ increases with reduced temperature, reflecting that by lowering the temperature the density of the finite-size-induced vortices is reduced and with that the conductivity increases. Thus, as conjectured, $f(T)$ in Eq. (10) depends on temperature. The agreement with Eq. (11), taking thermal fluctuations into account only, also reveals that around T_c the contribution of quantum fluctuations is negligibly small, although a nearly temperature-independent crossing point in the resistance-magnetic field plane occurs around $H_\perp\simeq5.5$ kOe.[30]

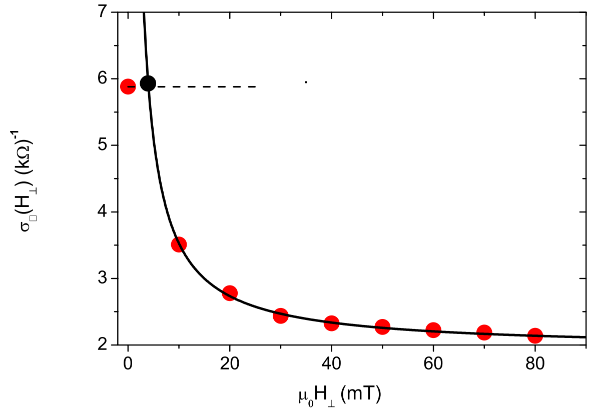

FIG. 6. (Color online) $\sigma_\square(T_c)$ vs $H_\perp$ for a $LaAlO_3/SrTiO_3$ interface with $T_c\simeq0.21$ K derived from Reyren *et al.* (Ref. 16). The solid line is Eq. (11) with $\sigma_n=1.94\times10^{-3}$ Ω and $f_\perp=1.59\times10^{-2}$ Ω mT. The dot marks $\mu_0H_\perp^\bullet=3.8$ mT.

The inset of Fig. 5 also reveals that $\sigma_\square(T)$ vs $H_\perp$ exhibits in the low-field limit a strong temperature dependence, weakening at higher fields. Noting that $\sigma_\square(T)$ vs $H_\parallel$ behaves in the same manner and the low-field behavior at T_c enters the determination of the limiting length $\hat{L}$ (see Figs. 3 and 4), a reliable estimation of $\hat{L}$ requires a good value of T_c. On the contrary, the parameters $f_\perp$ and $f_\parallel$ [Eq. (11)], determining the dynamical critical exponent z and the thickness d, do not vary much around T_c because there values are fixed in terms of the weakly temperature-dependent conductivities at higher magnetic fields.

To illustrate this tool further, allowing to determine z, d, and $\hat{L}$ from the magnetic field dependence of the conductivity at T_c we analyze the conductivity data of Reyren *et al.*[16] for a superconducting $LaAlO_3/SrTiO_3$ interface with $T_c\simeq0.21$ K. In Fig. 6 we show the sheet conductivity $\sigma_\square(T_c)$ vs $H_\perp$ derived from the resistivity data. Above $\mu_0H_\perp\simeq10$ mT we observe consistency with Eq. (11) for $z\simeq2$, in agreement with the value derived from *I-V* data,[14] and predicted for diffusive dynamics.[1] According to Fig. 7 and Eq. (11) $z\simeq2$ also follows from $\sigma(T_c)$ vs $H_\parallel$ above $\mu_0H_\parallel\gtrsim300$ mT. Given then the evidence for $z=2$ and the estimates for $f_\perp$ and $f_\parallel$ we obtain with Eqs. (12) and (19) for the thickness of the superconducting interface the value

$$d\simeq67 \text{ Å} \tag{21}$$

in agreement with previous estimates where $z=2$ was assumed.[16] Recently, room-temperature studies have also been performed to estimate the thickness of the $LaAlO_3/SrTiO_3$ interface grown at "high" oxygen pressures leading to a value of 70,[39] 100,[40] and 120 Å at 8 K.[41]

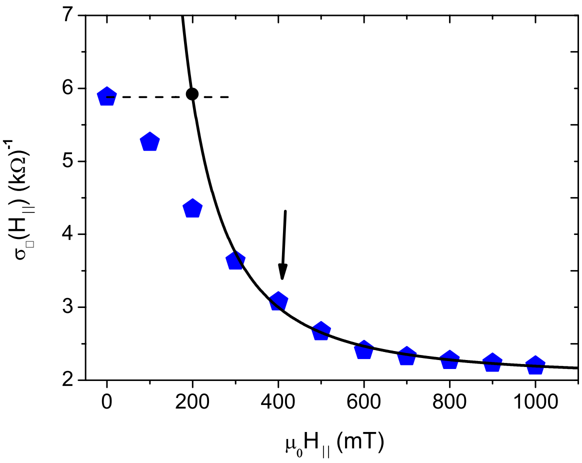

FIG. 7. (Color online) $\sigma(T_c)$ vs $H_\parallel$ for a $LaAlO_3/SrTiO_3$ interface with $T_c \simeq 0.21$ K derived from Reyren *et al.* (Ref. 16). The solid line is Eq. (11) with $\sigma_n = 2.04 \times 10^{-3}$ Ω and $f_\perp = 153.42$ Ω mT^2. The dot marks $\mu_0 H_\parallel^\bullet = 195$ mT.

Furthermore, in analogy to the amorphous $Nb_{0.15}Si_{0.85}$ film (see Figs. 3 and 4) $\sigma_\square(T_c)$ vs $H_{\perp,\parallel}$ does not diverge in the zero-field limit. This behavior was traced back to a standard finite-size effect, presumably attributable to a finite lateral extent $\hat{L}$ of the homogeneous domains.[17] To substantiate this interpretation we invoke Eq. (20) and the respective estimates for $H_\perp^\bullet$ and $H_\parallel^\bullet$, yielding with $a=4.8$ and $d \simeq 67$ Å, $\hat{L} \simeq 3.4 \times 10^{-5}$ cm$(\mu_0 H_\perp^\bullet = 3.8$ mT$)$ and $\hat{L} \simeq 4.9 \times 10^{-5}$ cm$(\mu_0 H_\parallel^\bullet = 195$ mT$)$, compared to the lateral dimensions $W \times L = 0.02$ cm$\times 0.01$ cm of the superconducting interface. Invoking the Nelson-Kosterlitz relation $\lambda_{2D}(T_c) = \lambda^2(T_c)/d = \Phi_0^2/(32\pi^2 k_B T_c)$,[21] we obtain $\lambda_{2D}(T_c) \simeq 4.8$ cm for $T_c = 0.21$ K, whereupon $\lambda_{2D} \gg \min[W,L]$ is well satisfied for the $LaAlO_3/SrTiO_3$ interface. Furthermore, because $\lambda_{2D}(T_c)$ is also large compared to $\hat{L}$, the zero-field limiting length appears to be set by the lateral extent of the homogenous domains. In any case due to the uncovered limiting length, not attributable a finite magnetic screening length λ_{2D}, it becomes possible for free vortices to form below T_c which in turn precludes a true phase transition.

In summary, we presented and illustrated a simple promising tool to extract from the magnetic field dependence of the conductivity at T_c the dynamical critical exponent z, the thickness d of thin superconducting films and interfaces, and the limiting length $\hat{L}$, giving rise to rounded BKT and QSI transitions even in zero field. In fact, in the quantum case is the divergence of the zero-temperature correlation length $\xi(T=0) = \bar{\xi}_0 \delta^{-\bar{\nu}}$ prevented because it cannot beyond $\hat{L}$ and with that is the attainable tuning regime bounded by $\delta > (\bar{\xi}_0/\hat{L})^{1/\nu}$.

The author is grateful to H. Aubin and C. A. Marrache-Kikuchi for providing the $Nb_{0.15}Si_{0.85}$ resistance data and N. Reyren, S. Gariglio, A. D. Caviglia, D. Jaccard, and J.-M. Triscone for providing the $LaAlO_3/SrTiO_3$ interface data. I also thank J.-M. Triscone, N. Reyren, S. Gariglio, A. D. Caviglia, and S. Weyeneth for fruitful conversations.

*tschnei@physik.unizh.ch

[1] D. S. Fisher, M. P. A. Fisher, and D. A. Huse, Phys. Rev. B **43**, 130 (1991).
[2] T. Schneider and J. M. Singer, *Phase Transition Approach to High Temperature Superconductivity* (Imperial College, London, 2000).
[3] S. W. Pierson, M. Friesen, S. M. Ammirata, J. C. Hunnicutt, and LeRoy A. Gorham, Phys. Rev. B **60**, 1309 (1999).
[4] K. Medvedyeva, B. J. Kim, and P. Minnhagen, Phys. Rev. B **62**, 14531 (2000).
[5] J. Holzer, R. S. Newrock, C. J. Lobb, T. Aouaroun, and S. T. Herbert, Phys. Rev. B **63**, 184508 (2001).
[6] D. R. Strachan, C. J. Lobb, and R. S. Newrock, Phys. Rev. B **67**, 174517 (2003).
[7] H. Jin and H.-H. Wen, Phys. Rev. B **68**, 094516 (2003).
[8] V. L. Berezinskii, Sov. Phys. JETP **32**, 493 (1971).
[9] J. M. Kosterlitz and D. J. Thouless, J. Phys. C **6**, 1181 (1973).
[10] V. Ambegaokar, B. I. Halperin, D. R. Nelson, and E. D. Siggia, Phys. Rev. B **21**, 1806 (1980).
[11] D. Finotello and F. M. Gasparini, Phys. Rev. Lett. **55**, 2156 (1985).
[12] Lindsay M. Steele, Ch. J. Yeager, and D. Finotello, Phys. Rev. Lett. **71**, 3673 (1993).
[13] D. R. Tilley and J. Tilley, *Superfluidity and Superconductivity* (Adam Hilger, Bristol, 1990).
[14] N. Reyren, S. Thiel, A. D. Caviglia, L. Fitting Kourkoutis, G. Hammerl, C. Richter, C. W. Schneider, T. Kopp, A.-S. Rüetschi, D. Jaccard, M. Gabay, D. A. Muller, J.-M. Triscone, and J. Mannhart, Science **317**, 1196 (2007).
[15] A. D. Caviglia, S. Gariglio, N. Reyren, D. Jaccard, T. Schneider, M. Gabay, S. Thiel, G. Hammerl, J. Mannhart, and J.-M. Triscone, Nature (London) **456**, 624 (2008).
[16] N. Reyren, S. Gariglio, A. D. Caviglia, D. Jaccard, T. Schneider, and J.-M. Triscone, Appl. Phys. Lett. **94**, 112506 (2009).
[17] T. Schneider, A. D. Caviglia, S. Gariglio, N. Reyren, and J.-M. Triscone, Phys. Rev. B **79**, 184502 (2009).
[18] V. Privman, in *Finite Size Scaling and Numerical Simulations of Statistical Systems*, edited by V. Privman (World Scientific, Singapore, 1990).
[19] J. Pearl, Appl. Phys. Lett. **5**, 65 (1964).
[20] M. R. Beasley, J. E. Mooij, and T. P. Orlando, Phys. Rev. Lett. **42**, 1165 (1979).
[21] D. R. Nelson and J. M. Kosterlitz, Phys. Rev. Lett. **39**, 1201 (1977).
[22] M. Tinkham, *Introduction to Superconductivity*, 2nd ed. (Dover, New York, 1996).
[23] J. Barnas and I. Weymann, J. Phys.: Condens. Matter **20**, 423202 (2008).
[24] K. Kim and H. J. Lee, Phys. Rev. B **54**, 13152 (1996).
[25] N. Marković, C. Christiansen, A. M. Mack, W. H. Huber, and A.

M. Goldman, Phys. Rev. B **60**, 4320 (1999).
[26] V. F. Gantmakher, M. V. Golubkov, V. T. Dolgopolov, G. E. Tsydynzhapov, and A. A. Shashkin, JETP Lett. **71**, 160 (2000).
[27] N. Mason and A. Kapitulnik, Phys. Rev. B **64**, 060504(R) (2001).
[28] E. Bielejec and W. Wu, Phys. Rev. Lett. **88**, 206802 (2002).
[29] A. M. Goldman, Physica E (Amsterdam) **18**, 1 (2003).
[30] H. Aubin, C. A. Marrache-Kikuchi, A. Pourret, K. Behnia, L. Bergé, L. Dumoulin, and J. Lesueur, Phys. Rev. B **73**, 094521 (2006).
[31] M. A. Steiner, N. P. Breznay, and A. Kapitulnik, Phys. Rev. B **77**, 212501 (2008).
[32] S. L. Sondhi, S. M. Girvin, J. P. Carini, and D. Shahar, Rev. Mod. Phys. **69**, 315 (1997).
[33] R. Crane, N. P. Armitage, A. Johansson, G. Sambandamurthy, D. Shahar, and G. Grüner, Phys. Rev. B **75**, 184530 (2007).
[34] A. Aharony and A. B. Harris, Phys. Rev. Lett. **77**, 3700 (1996).
[35] B. I. Halperin and D. R. Nelson, J. Low Temp. Phys. **36**, 599 (1979).
[36] L. G. Aslamosov and A. I. Larkin, Sov. Phys. Solid State **10**, 875 (1968).
[37] A. Larkin and A. Varlamov, *Theory of Fluctuations in Superconductors* (Clarendon, Oxford, 2005).
[38] C. A. Marrache-Kikuchi (private communication).
[39] M. Basletić, J.-L. Maurice, C. Carrétéro, G. Herranz, O. Copie, M. Bibes, É. Jacquet, K. Bouzehouane, S. Fusil, and A. Barthélémy, Nature Mater. **7**, 621 (2008).
[40] M. Sing, G. Berner, K. Goss, A. Muller, A. Ruff, A. Wetscherek, S. Thiel, J. Mannhart, S. A. Pauli, C. W. Schneider, P. R. Willmott, M. Gorgoi, F. Schafers, and R. Claessen, Phys. Rev. Lett. **102**, 176805 (2009).
[41] O. Copie, V. Garcia, C. Bödefeld, C. Carrétéro, M. Bibes, G. Herranz, E. Jacquet, J.-L. Maurice, B. Vinter, S. Fusil, K. Bouzehouane, H. Jaffrès, and A. Barthélémy, Phys. Rev. Lett. **102**, 216804 (2009).